Electronic Supplementary Material (ESI) for RSC Advances.
This journal is © The Royal Society of Chemistry 2018

Supporting Information

# $Ag_3PO_4$ Electrocatalyst for Oxygen Reduction Reaction: Enhancement from Positive Charge

*Yong Qin,*[†,#] *Fan Li,*[†,#] *Peng Tu,*[‡,#] *Yanling Ma,*[†] *Wenlong Chen,*[†] *Fenglei Shi,*[†] *Qian Xiang,*[†] *Hao Shan,*[†] *Lifu Zhang,*[†] *Peng Tao,*[†] *Chengyi Song,*[†] *Wen Shang,*[†] *Tao Deng,*[†] *Hong Zhu,**[,†,‡,§] *Jianbo Wu,**[†,§]

[†]State Key Laboratory of Metal Matrix Composites, School of Materials Science and Engineering, Shanghai Jiao Tong University, 800 Dongchuan Rd, Shanghai, 200240, People's Republic of China.

[‡]University of Michigan – Shanghai Jiao Tong University Joint Institute, Shanghai Jiao Tong University, 800 Dongchuan Road, Shanghai, 200240, P. R. China

[§]Materials Genome Initiative Center, Shanghai Jiao Tong University, 800 Dongchuan Road, Shanghai, 200240, P. R. China

*E-mail: jianbowu@sjtu.edu.cn

*E-mail: hong.zhu@sjtu.edu.cn

#These authors contribute equally to this work

Correspondence and requests for materials should be addressed to J. B. Wu, H. Zhu

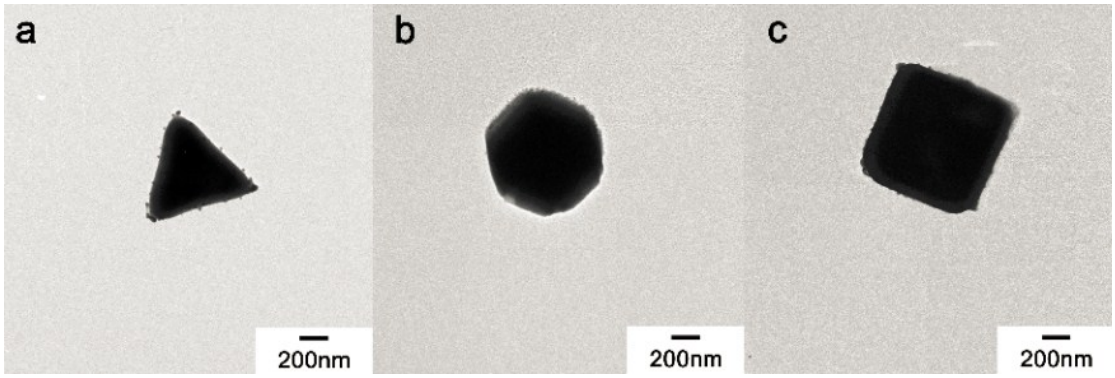


**Figure S1.** TEM micrograph of $Ag_3PO_4$ crystals (a) tetrahedron, (b) rhombic dodecahedron, (c) cube

As shown in **Figure S1**, $Ag_3PO_4$ tetrahedron, rhombic dodecahedron, and cube with regular structures have been fabricated. These three types' plane projection draws are triangle, hexagon and quadrangle, respectively. These results are consistent with the SEM images of crystals in Figure 1.

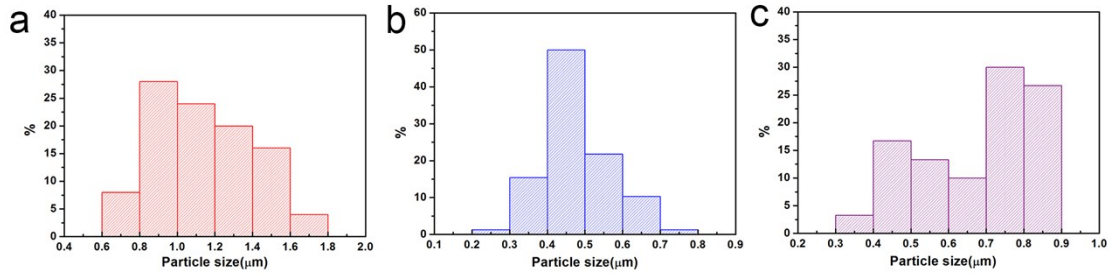


**Figure S2.** Particle size distribution of $Ag_3PO_4$ with different facets: (a) tetrahedron (b) rhombic dodecahedron (c) cube.

The size distribution of $Ag_3PO_4$ with different facets is counted according to SEM micrographs of different $Ag_3PO_4$ crystals. The particle sizes follow a normal distribution as shown in **Figure S2**. And the average size is applied to the calculation of atomic activity about different $Ag_3PO_4$ crystals.

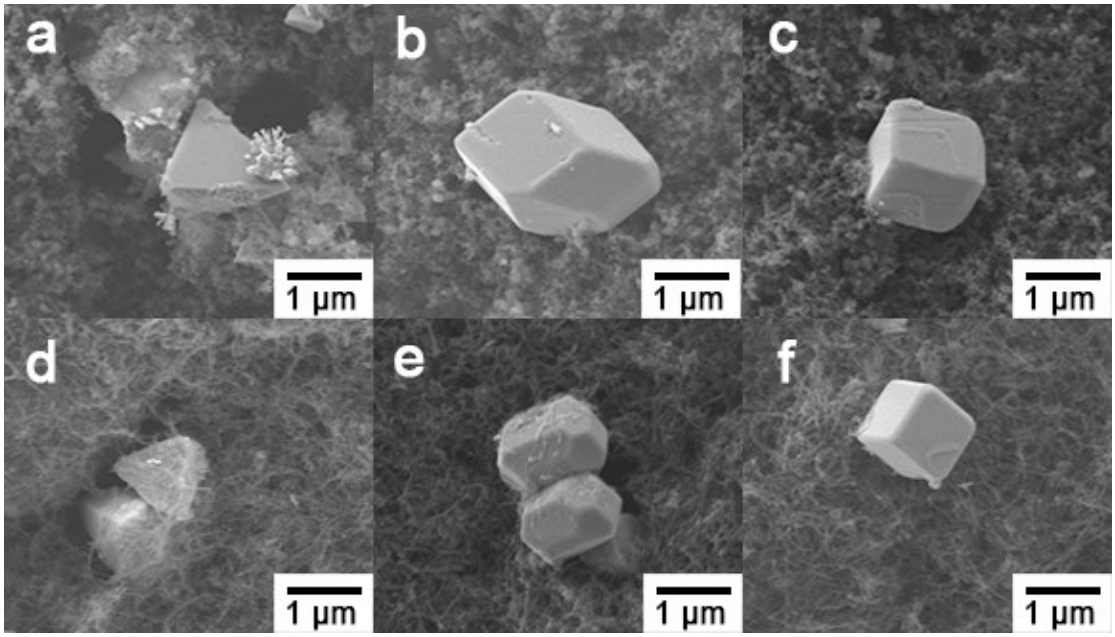


**Figure S3.** SEM micrograph of (a, b, c) $Ag_3PO_4$/C and (d, e, f) $Ag_3PO_4$/CNT. (a, d) tetrahedron; (b, e) rhombic dodecahedron; (c, f) cube

Figure S3 shows the SEM images of $Ag_3PO_4$/C and $Ag_3PO_4$/CNT. We can find that the carbon is amorphous, while the carbon nanotube is slender tubular. And the $Ag_3PO_4$ crystals with different facet were dispersed in carbon and carbon nanotube, respectively.

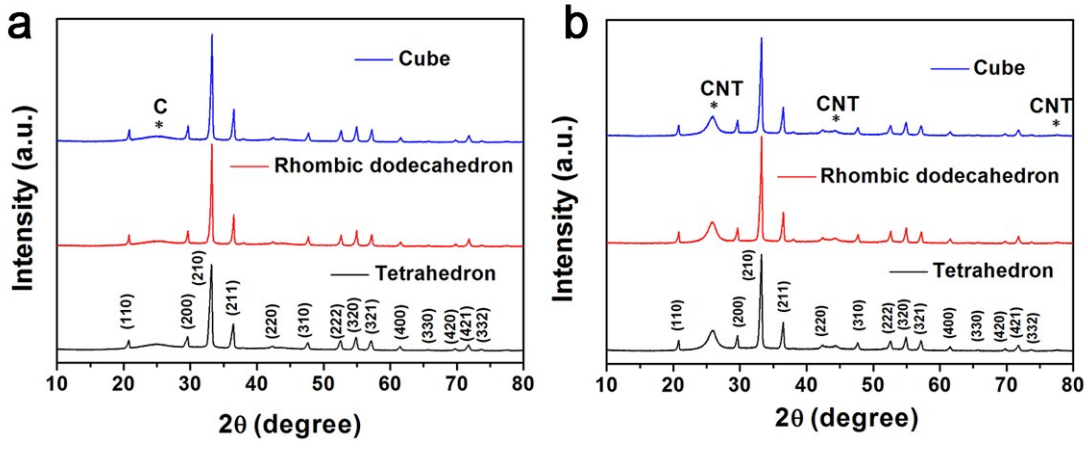


**Figure S4.** XRD pattern of (a) $Ag_3PO_4$/C and (b) $Ag_3PO_4$/CNT.

The XRD pattern shows that all of the diffraction peaks could be indexed to $Ag_3PO_4$/C (Figure S4a) and $Ag_3PO_4$/CNT (Figure S4b).

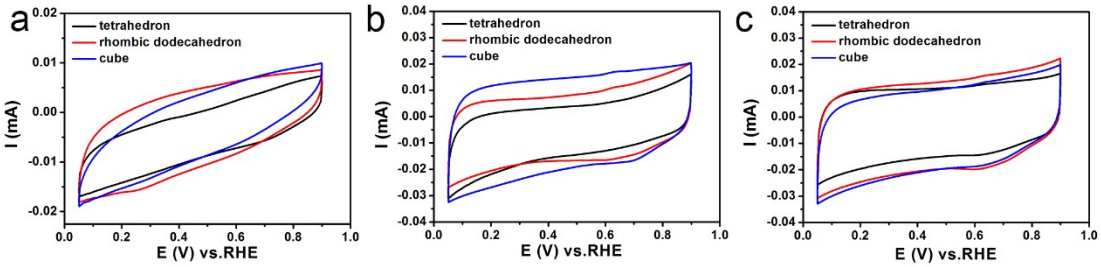


**Figure S5.** CV curves of tetrahedral, rhombic dodecahedral and cubic $Ag_3PO_4$ catalysts (a) pure $Ag_3PO_4$, (b) $Ag_3PO_4$/C, (c) $Ag_3PO_4$/CNT. The mass of $Ag_3PO_4$ is 10 μg

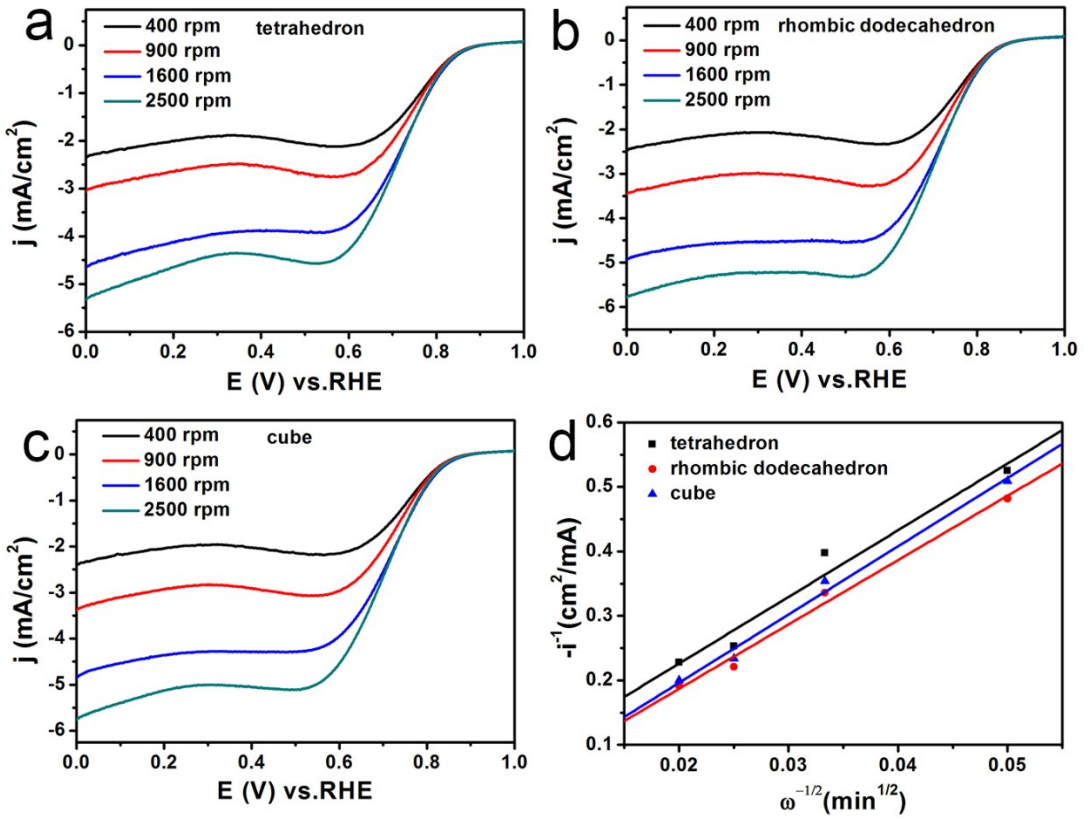


**Figure S6.** RDE voltammograms for the ORR of (a) tetrahedral, (b) rhombic dodecahedral and (c) cubic, $Ag_3PO_4$/CNT electrocatalysts at various rotation rates, (d) Koutecky–Levich plots of the rotating disk current at 0.3 V (vs. RHE). The tests were conducted in $O_2$-saturated 0.1 M KOH solution and the scan rate was kept at 10 mV/s

Meanwhile, we test the $Ag_3PO_4$/CNT catalysts ORR performance of rotation speed of RDE from 400 to 2500 rpm shown as **Figure S4**. From the ORR curve, the numerical value of n was calculated to be 2.8, 2.9 and 2.7, respectively, for tetrahedral, rhombic dodecahedral and cubic of $Ag_3PO_4$/CNT catalysts at 0.3V (vs. RHE).

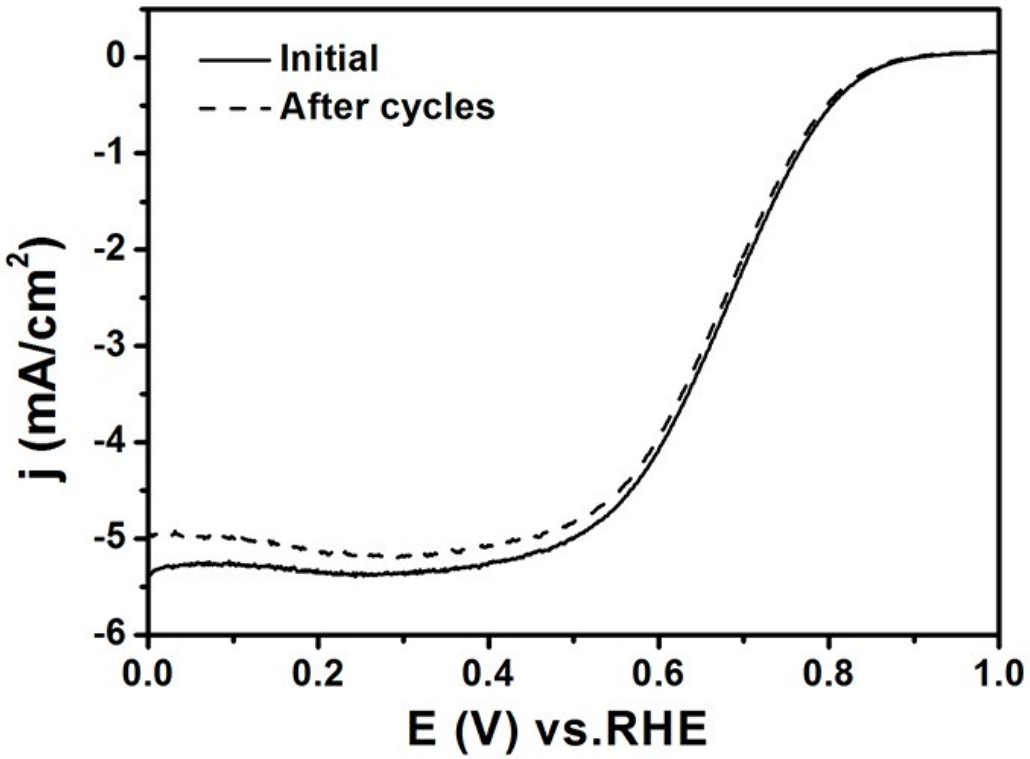


Figure S7. ORR stability of as-prepared $Ag_3PO_4$/CNT catalyst after 5000 cycles.

The long-term stability of catalyst was evaluated through accelerated durability test (ADT) by applying cyclic potential sweep between 0.6 and 1.0 V vs.RHE in an Ar-saturated 0.1 M KOH solution at room temperature. We can obtain the reduced 12.5% mass activity from Figure S7 after 5000 cycles.

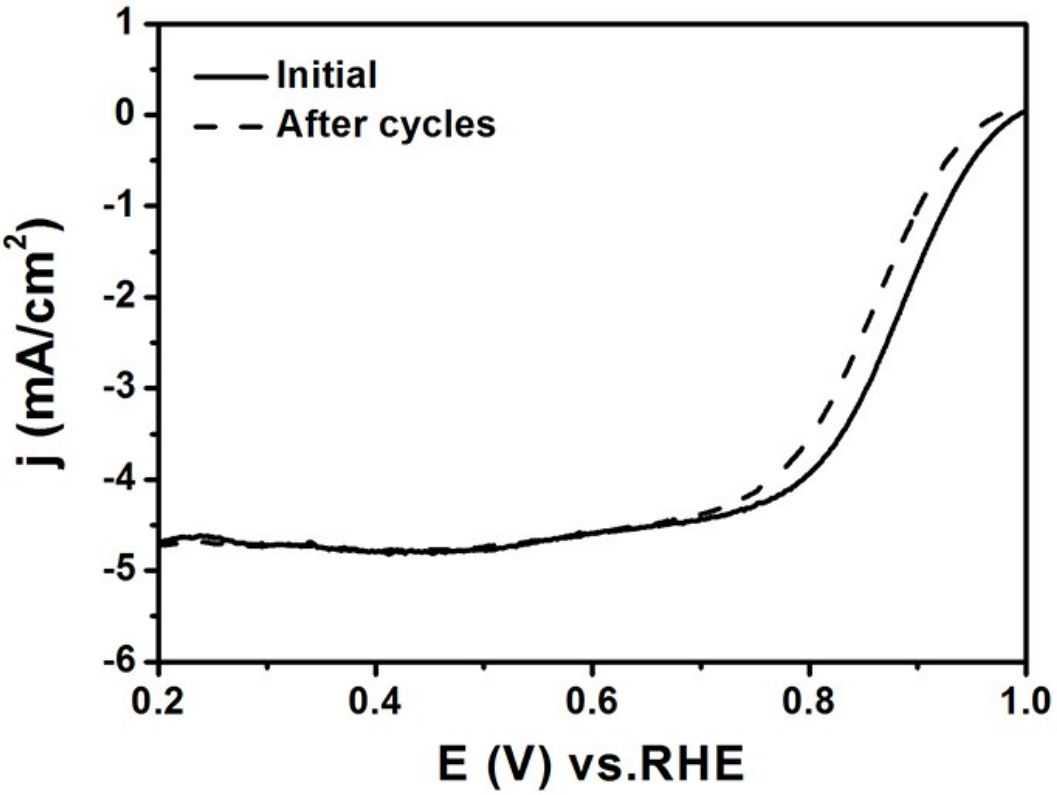


Figure S8. ORR stability of commercial Pt/C catalyst after 5000 cycles.

After 5000 cycles, the mass activity of commercial Pt/C was reduced 36% from Figure S8. Compared to commercial Pt/C, the rhombic dodecahedral $Ag_3PO_4$/CNT catalyst possesses better stability.

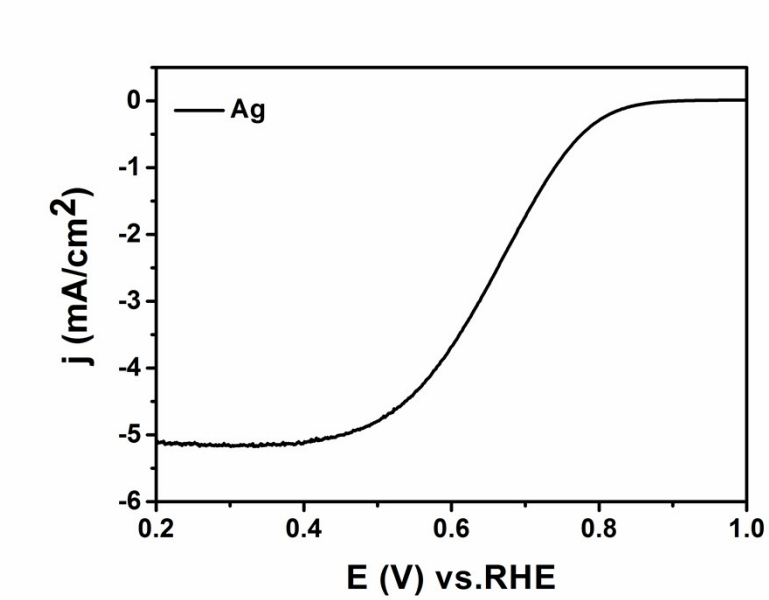


**Figure S9**. ORR Polarization curve of Ag in 0.1 M KOH

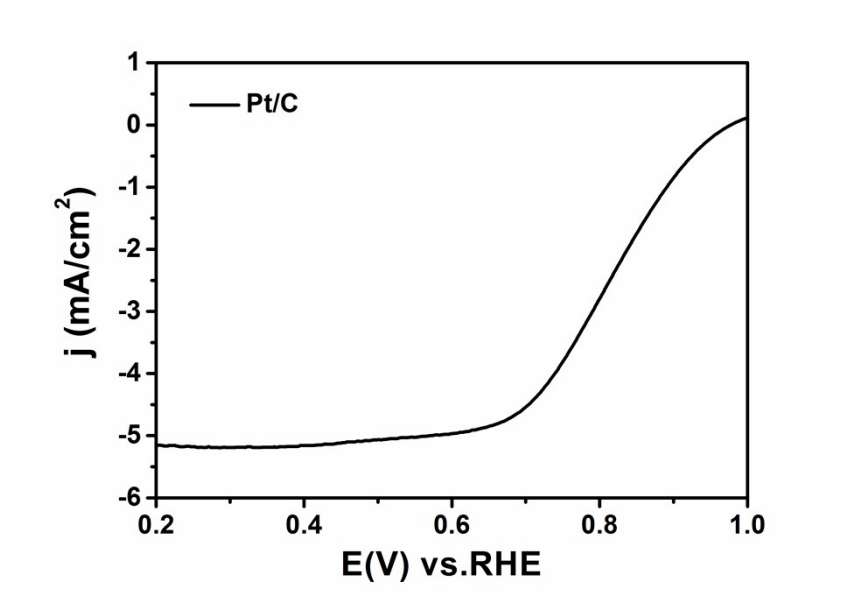


**Figure S10.** ORR polarization curve of Pt/C in 0.1 M KOH.

**Table S1.** Kinetic current ($I_k$) of Ag, Pt/C catalysts in 0.1 mol/L KOH.

| Sample | Metal loading(μg) | $I_k$(mA) | Mass activity (mA/μg) at 0.8 V |
|---|---|---|---|
| Ag | 10 | 0.06070 | 0.00607 |
| Pt/C | 8 | 1.19600 | 0.14950 |

**Table S2.** Atomic activity and relevant parameters

| Facet | $Ag_3PO_4${111} | $Ag_3PO_4${110} | $Ag_3PO_4${100} |
|---|---|---|---|
| Average size(nm) | 1140 | 478.2 | 676.7 |
| Shape | tetrahedron | rhombic dodecahedron | cube |
| Volume of single crystal(Å3), $V$ | $1.7460\times10^{11}$ | $3.3672\times10^{11}$ | $3.0988\times10^{11}$ |
| Density of $Ag_3PO_4$(g/cm$^3$), $\rho$ | 6.08 | 6.08 | 6.08 |
| Total Ag Atoms in single crystal, $Ag_{total}$ | $1.75\times10^{9}$ | $6.51\times10^{9}$ | $3.31\times10^{9}$ |
| Surface area of single crystal (Å$^2$), $Ag_{surface}$ | $2.251\times10^{8}$ | $2.587\times10^{8}$ | $2.748\times10^{8}$ |
| Ag atom density(atom/Å$^2$), $\omega$ | 0.046305 | 0.075615 | 0.053468 |
| Outmost Ag atomic ratio(%), $i$ | 0.228 | 0.222 | 0.181 |
| Loading of $Ag_3PO_4$(μg), $m$ | 10 | 10 | 10 |
| Total Ag Atoms, $Ag_{loading}$ | $4.31608\times10^{16}$ | $4.31608\times10^{16}$ | $4.31608\times10^{16}$ |
| Ag atoms involved in the reaction, $Ag_{involed}$ | $1.35525\times10^{14}$ | $1.05744\times10^{14}$ | $1.04017\times10^{14}$ |
| Kinetic current(mA), $I_k$ | 0.0359 | 0.0431 | 0.0270 |
| Atomic activity (mA/atom$_{Ag}$), $i_{k,atom}$ | $3.65137\times10^{-16}$ | $4.50425\times10^{-16}$ | $3.45801\times10^{-16}$ |

**Table S2** shows the relevant parameters of calculation of atomic activity. According to particle size distribution of $Ag_3PO_4$ with different facets, we can obtain the average size. Combined with the shape, the volume of single crystal is received. So that Ag atomic ratio on the surface can be obtained according to following formula:

$$Ag_{total} = \frac{\rho \cdot V}{M_{Ag_3PO_4}} \cdot N_A \cdot 3 \quad (1)$$

$$Ag_{surface} = S \cdot \omega \quad (2)$$

$$i = \frac{Ag_{surface}}{Ag_{total}} \times 100\% \quad (3)$$

where $Ag_{total}$ is the total number of Ag atoms in single crystal, $\rho$ is density of $Ag_3PO_4$, $V$ is the volume of single crystal, $M_{Ag_3PO_4}$ is molecular weigh of $Ag_3PO_4$, $N_A$ is Avogadro's number, $Ag_{surface}$ means the number of outmost Ag atoms on the surface of single crystal, $S$ is the surface area of single crystal, $\omega$ is the surface Ag atom denity, $i$ means outmost Ag atomic ratio.

The loading mass of $Ag_3PO_4$ is 10 μg, which means the loading of Ag and the number of Ag atoms involved in the reaction can be received. Assume that all Ag atoms on the surface are involved in the reaction, so the catalytic atomic activity of single Ag atom on the surface can be calculated according to the following formula:

$$Ag_{loading} = \frac{m}{M_{Ag_3PO_4}} \cdot 3 \quad (4)$$

$$Ag_{involed} = Ag_{loading} \cdot i \quad (5)$$

$$i_{k,atom} = \frac{I_K}{Ag_{involed}} \quad (6)$$

where $Ag_{loading}$ is the total number of Ag atoms of loading on the RDE, $m$ is the loading mass of $Ag_3PO_4$, $Ag_{involed}$ is the number of Ag surface atoms involved in the reaction, $I_k$ is kinetic current, $i_{k,atom}$ is catalytic atomic activity of single Ag atom on the surface.

**Table S3.** Atomic activity and parameters of pure Ag

| Materials | Pure Ag |
|---|---|
| Average size (nm) | 23.7 |
| Kinetic current(mA), $I_k$ | 0.0607 |
| Atomic activity (mA/atom$_{Ag}$), $i_{k,atom}$ | $5.99961\times10^{-17}$ |

**Computational Method**

The density functional theory (DFT) calculations with the Perdew-Burke-Ernzerhof (PBE)[1] generalized gradient approximation (GGA) and projector augmented wave (PAW)[2] pseudopotentials were performed within the Vienna Ab Initio Simulation Package (VASP). For all $Ag_3PO_4$ slabs considered, namely {111}, {110}, and {100} surfaces, the energy cut-off for the plane wave expansion of 520 eV, a 4*2*1 k-point mesh and a vacuum region of 20 Å were used.

To study the O adsorption on the three surfaces, we placed the O atom onto the 2*1 slabs. For each slab with adsorbate, several possible adsorption sites were considered, including top, bridge, and hollow (see Figure 5 and **Table S4** for more details).

The absorption energy ($E_{ads}$) is calculated from the total energy difference between the slab with the adsorbate ($E_{Ag3PO4-O}$), the slab without the adsorbate ($E_{Ag3PO4}$), and the adsorbate in the gas phase ($E_{O2}$). Therefore, the adsorption energy can be written as

$$E_{ads} = E_{Ag_3PO_4-O} - E_{Ag_3PO_4} - \frac{1}{2}E_{O_2} \quad (7)$$

The preferential adsorption energy for $Ag_3PO_4$ {111}, {110}, and {100} surfaces, i.e. the adsorption energy for most favored adsorption site, is -2.151 eV, -0.830 eV, -

2.996 eV, respectively. The most preferential adsorption sites are bolded in Table S4. Our volcano plot combining the adsorption energy and atomic activity is shown in Figure 4e. It's obvious that the number of the stable site in one slab accounts for the highest proportion.

**Table S4.** Adsorption energy for O on $Ag_3PO_4$ {111}, {110} and {100}.

| Surface Orientation | Adsorption sites | $E_{ads}$ |
|---|---|---|
| {111} | Ag-top | **-2.151** |
| | Ag-Ag_bridge1 | 1.834 |
| | Ag-Ag_bridge2 | 2.424 |
| | Ag_hollow1 | 2.050 |
| Surface Orientation | Adsorption sites | $E_{ads}$ |
| {110} | Ag_top1 | 1.925 |
| | Ag_top2 | **-0.830** |
| | Ag_top3 | 1.232 |
| | Ag_top4 | 4.292 |
| | Ag-Ag_bridge1 | -0.011 |
| | Ag-Ag_bridge2 | 2.254 |
| | Ag-Ag_bridge3 | -0.426 |
| | Ag-Ag_bridge4 | 4.574 |
| Surface Orientation | Adsorption sites | $E_{ads}$ |
| {100} | Ag_top | 0.642 |
| | P_top | 2.163 |
| | Ag-Ag_bridge | 0.016 |
| | P-P_bridge1 | 0.822 |
| | P-P_bridge2 | 2.775 |
| | P-Ag_bridge | **-2.996** |

Note: 1. Preferential adsorption sites are bolded.
2. All the units of energies are eV.

**Table S5.** Adsorption energy for O on pure Ag

| Adsorption sites | $E_{ads}$ |
|---|---|
| bridge | -0.243 |
| fcc | -0.398 |
| hcp | **-0.493** |
| top | 1.058 |

## Reference：


1 J. P. Perdew, K. Burke and M. Ernzerhof, *Phys. Rev. Lett.*, 1997, **78**, 1396-1396.

2 P. E. Blöchl, O. Jepsen and O. K. Andersen, *Physical Review B*, 1994, **49**, 16223-16233.